Research Article

Dwi Hudiyanti*, Salma Nur Hidayati, Parsaoran Siahaan, Ngadiwiyana Ngadiwiyana, Abidin Nur, Ratna Indria Sari, Indrian Rizka Amalia, Sherllyn Meida Christa, Amanda Chindy Patrechia, Adinda Eka Maharani

Impact of cholesterol in encapsulated vitamin E acetate within cocoliposomes

https://doi.org/10.1515/chem-2024-0122
received May 29, 2024; accepted November 15, 2024

Abstract: Vitamin E acetate (VEA) is commonly used in manufacturing pharmaceuticals, food additives, and animal feeds. However, VEA possesses disadvantages, including low water solubility, low bioavailability, and susceptibility to degradation and oxidation. This study investigated the use of cocoliposomes for encapsulating VEA (VEACL). The cocoliposomes consisted of coconut phospholipids (CocoPLs) and cholesterol (Chol). Several parameters, such as functional groups, transition temperature, encapsulation efficiency (EE), release profile, particle size, polydispersity index, and zeta potential, were analyzed to evaluate the impact of cholesterol inclusion on the cocoliposome membrane. The results show that the Fourier transform infrared spectra of VEACL do not exhibit any new, distinct peaks that differ from the peaks of its constituent composition. Therefore, it confirmed that no chemical reactions occurred during the manufacturing of VEACL. Cholesterol in the system raises the transition temperature of phospholipids and enhances the stability of VEACL. The EE remains above 80% despite a 20% increase in cholesterol levels. The release rate of VEA from cocoliposomes was slower with VEACL–20%Chol compared to VEACL–0%Chol. The cholesterol level leads to a decrease in particle size and an increase in the negative zeta potential of the cocoliposomes. Data show that cocoliposomes are effective carriers for VEA encapsulation.

Keywords: encapsulation efficiency, differential scanning calorimeter, release rate, particle size, zeta potential, thermal analysis

*** Corresponding author: Dwi Hudiyanti,** Department of Chemistry, Faculty of Sciences and Mathematics, Diponegoro University, Semarang, 50275, Indonesia, e-mail: dwi.hudiyanti@live.undip.ac.id
Salma Nur Hidayati, Sherllyn Meida Christa, Amanda Chindy Patrechia, Adinda Eka Maharani: Chemistry Program, Faculty of Sciences and Mathematics, Diponegoro University, Semarang, 50275, Indonesia
Parsaoran Siahaan, Ngadiwiyana Ngadiwiyana: Department of Chemistry, Faculty of Sciences and Mathematics, Diponegoro University, Semarang, 50275, Indonesia
Abidin Nur, Ratna Indria Sari, Indrian Rizka Amalia: Research Center for Fishery, National Research and Innovation Agency, Bogor, Indonesia

1 Introduction

Vitamin E acetate (VEA), sometimes referred to as α-tocopheryl acetate, is classified as a fat-soluble vitamin and is recognized for its strong antioxidant properties. VEA is a synthetic or ester form of vitamin E (VE; α-tocopherol) that is commonly employed due to its superior stability [1–3]. VEA has a longer shelf life than VE due to its lower acidity resulting from the presence of blocked phenolic hydroxyl groups [4]. Upon ingestion, VEA undergoes hydrolysis in the body, resulting in the formation of VE and acetic acid. This process allows the retention of advantages similar to those of VE. When applied topically in skincare or cosmetics, VEA offers superior antioxidant benefits compared to VE. This is because VEA is more effective in preventing the formation of harmful peroxides on the skin. Additionally, VEA's less acidic nature allows it to be absorbed into the skin without rapid hydrolysis. VEA has several benefits, such as (i) safeguarding cellular and intracellular membranes, polyunsaturated fatty acids, and lipoprotein from oxidative damage [3,5]; (ii) shielding the skin from detrimental effects caused by external harmful substances, such as sunlight, pollution, and chemicals, by inhibiting the formation of free radicals [2]; (iii) reducing DNA damage and mortality rates in keratinocytes; and (iv) enhancing the hydration of the stratum corneum (the outermost layer of the epidermis) [6]. Antioxidants from VEA have extensive use in dietary supplements and fortified foods for animals, in addition to humans [7–12]. This is because VEA exhibits resistance to oxidation, allowing the feed to remain stable for a longer period of time during storage [4].

Despite the advantages it offers, VEA has inherent limitations that need to be addressed to fully harness its

potential benefits. VE exhibits a high oral bioavailability of approximately 50–80% upon consumption, unlike its esterified form, VEA. Despite VEA's greater stability compared to free VE, its bioavailability is significantly affected by intestinal absorption, hepatic metabolism, and cellular excretion, as its absorption adheres to the general absorptive route of dietary fats [13–15]. Qureshi et al. [16] investigated the pharmacokinetics of δ-tocotrienol to ascertain the pharmacokinetics and bioavailability of all eight isomers of tocotrienols and tocopherols isolated from human plasma samples, revealing that only a small amount of VEA is fully absorbed by the body. Following the administration of three separate single doses to a group of healthy males – 125 mg, 250 mg, and 500 mg – the peak plasma concentrations recorded 6 h post-ingestion were 1,822 ± 48.24 μg/mL, 1,931 ± 92.54 μg/mL, and 2,188 ± 147.61 μg/mL, respectively. The observed volume of distribution (Vd) values from three single administered doses in the same participants were 0.070 ± 0.0002 mL, 0.127 ± 0.004 mL, and 0.232 ± 0.010 mL, respectively. The Vd in pharmacokinetic parameters signifies a drug's propensity to persist in the plasma or to be redistributed to various tissue compartments in the body. A low Vd signifies that the drug predominantly resides in the plasma, necessitating a reduced dosage to attain a specific plasma concentration adequate for distribution to other bodily tissues [17,18]. The absorption of VEA in the body is deemed less efficient than other lipids, as VEA must first undergo hydrolysis by the lipase enzyme, which relies on bile acids from the pancreas or by intestinal mucosal esterase. Subsequently, it can be absorbed by intestinal cells by the transfer of emulsified fat globules to multi- and unilamellar vesicles that are water-soluble, accompanied by mixed micelles composed of phospholipids and bile acids [13]. Consequently, the low bioavailability of VEA in the body is influenced by several factors: (i) its esterified form necessitates hydrolysis in the intestine to release its free form for absorption [14,19], (ii) the route of administration (oral versus injection) [3], and (iii) the internal absorption of VEA into enterocytes requires lipid-rich foods [13]. The vulnerability also lies in its ability to dissolve. Both VE and VEA, being fat-soluble molecules, exhibit low solubility in water [20]. Applying VEA to a product in a water-dominated environment poses a significant obstacle. Hence, in order to address the issue of VEA solubility, it is crucial to modify the packaging in terms of methods, types, and/or sizes. The packaging methods of VE and VEA using capsules, balls or vesicles, emulsions, and a range of sizes from macro to nano have been studied [21–24]. Below are several studies that have utilized different methods, types, and sizes of packaging to encapsulate VE and/or VEA, including (i) mixed micelles with the emulsion titration method to encapsulate VE and VEA [1]; (ii) microcapsules with the spray-drying method to encapsulate VE and VEA [25,26]; (iii) nano-emulsions with the oil-in-water emulsification method to encapsulate VE [26]; (iv) lipid nano-capsules with the phase-inversion temperature method and nano-structured lipid carriers with the emulsification-solvent diffusion method, both to encapsulate VE [27]; (v) liposomes with the thin-film hydration method to encapsulate VEA [28]; (vi) edible emulsion stabilized with natural food-grade surfactant with the oil-in-water emulsification method to encapsulate VE [29]; (vii) emulsion gels stabilized by polysaccharides and modified shea butter to encapsulate VEA [30]; and (viii) microbeads with oil-in-water emulsification and solvent evaporation methods to encapsulate VEA [31].

Liposomes are a versatile type of lipid-based packaging commonly used as a drug delivery system (DDS) to carry drugs, whether they are hydrophilic (water-soluble) or lipophilic (fat-soluble), to target cells in the body [32,33]. Liposomes are widely recognized for their potential to enhance the solubility, stability, and bioavailability of lipophilic drugs, making them a considerable option in DDS [34–36]. Liposomes possess a spherical vesicle structure with a closed form, containing an aqueous compartment that is enveloped by bilayers of phospholipids [37]. This shape facilitates the utilization of liposomes as DDS, where the aqueous compartment can accommodate hydrophilic molecules while the bilayers of phospholipids can encapsulate lipophilic molecules [33]. Liposomes can be modified to nanoscale sizes, which increases their versatility as carriers of drugs [37,38]. Multiple studies undertaken by numerous researchers have demonstrated that liposomes can be enhanced with diverse molecules to augment their efficacy as carriers in DDS [32,38–40]. Liposomes primarily consist of phospholipids, which are amphiphilic molecules capable of self-assembly in aqueous environments [33,41]. Phospholipids, which are the primary building blocks of the cell membrane, have advantageous features for liposomes, including being non-toxic, biodegradable, biocompatible, and non-immunogenic upon entering the body [35,37,39]. Phospholipids, which are the primary components of cell membranes, are readily available in both natural and synthetic forms. Phospholipids can be obtained by extracting them from several sources, including soybeans, jack beans, egg yolks, sunflowers, rice bran, sesame, and coconut. The high concentration of phospholipids in coconuts, combined with their widespread availability in nature, makes them an excellent choice as a primary material for producing liposomes. Prior studies have demonstrated the efficacy of liposomes derived from coconut phospholipids extracts (CocoPLs) in encapsulating hydrophilic drugs, namely vitamin C [42]. The potential

of encapsulating drugs in liposomes is significant in various areas, including the food industry, pharmaceuticals, and cosmetics [21,23,33,37]. Consequently, numerous studies and advancements are currently dedicated to the encapsulation of drugs within liposomes and/or nanoliposomes for diverse objectives. Hudiyanti et al. [42,43] conducted multiple studies on the use of CocoPL-based liposomes (cocoliposomes) as DDS for different drugs. Hence, cocoliposomes possess the capability to serve as DDS for VEA. However, there has been no research on the specific topic of VEA encapsulation in liposomes using CocoPL precursors. Hence, the objective of this study is to develop and study the effectivity of cocoliposomes as a DDS for VEA. Furthermore, this study aims to investigate the impact of including cholesterol as a stabilizer in the liposome membrane on the outcomes of VEA encapsulation within cocoliposomes (VEACL). The results of our study demonstrate that cholesterol has several impacts on the properties of VEACL, as indicated by the changes observed in the zeta potential, particle size, polydispersity index (PI), and transition temperature. The observed results include an increase in the temperature at which phospholipid transition occurs, a reduction in the encapsulation efficiency (EE) of VEA while still maintaining a satisfactory percentage of successful encapsulation, particularly above 80% in the presence of high cholesterol (40%), a decrease in liposome leakage levels, and an improvement in the stability of VEACL.

2 Materials and methods

2.1 Reagents and chemicals

The materials used in this study are ripe coconut (*Cocos nucifera L.*), chloroform p.a. (Merck KGaA, Darmstadt, Germany), methanol p.a. (Merck KGaA, Darmstadt, Germany), technical 87% (*v*/*v*) ethanol (Kimia Kalijaga, Demak, Indonesia), technical *n*-hexane (Kimia Kalijaga, Demak, Indonesia), $Na_2HPO_4{\cdot}2H_2O$ p.a. (Merck KGaA, Darmstadt, Germany), $NaH_2PO_4{\cdot}2H_2O$ p.a. (Merck KGaA, Darmstadt, Germany), NaCl p.a. (HiMedia, PA, USA), α-tocopherol acetate (VEA) powder p.a. (90%; DSM, Heerlen, Netherlands), cholesterol (Chol) p.a. (94%; Sigma-Aldrich, Darmstadt, Germany), 0.1 M HCl p.a., 0.1 M NaOH p.a., demineralized water (Brataco, Semarang, Indonesia), and nitrogen gas.

2.2 Isolation of coconut phospholipids (CocoPLs)

The isolation of coconut phospholipids (CocoPLs) was performed with a slight modification of Hudiyanti's method [43]. The process began with sample preparation, which involved peeling and cleaning the ripe coconut meat. The meat was then subjected to a dehydrator at 40°C for 6 h. Subsequently, the dried coconut meat was ground into a fine powder using a chopper, and the resulting powder was further processed using a press machine to separate the pulp and oil. A modification to the prior method involved employing an ultrasonic homogenizer for maceration. About 100 g of coconut pulp was macerated in a 400 mL solvent mixture of chloroform p.a. and methanol p.a. (in a ratio of 2:1, v/v) using an ultrasonic homogenizer (50% pulser, 80% power, 3 × 15 min, 360 rpm stirring). The maceration product was subsequently filtered through two layers of filter paper, washed with a 0.9% NaCl p.a. solution, and then evaporated to get a crude lipid extract. The process of isolating phospholipids was continued with partition extraction using solvent A (technical *n*-hexane), which was saturated with solvent B (technical 87% (v/v) ethanol). The ratio of the volume of crude extract to solvent A to solvent B was 2:9:3 (v/v/v). The method involved combining 100 mL of crude lipid extract with 450 mL of solvent A, stirring for 3 min, and subsequently adding and stirring 150 mL of solvent B. The mixture was then partitioned using two separatory funnels. The lower phase was separated and mixed with solvent A and then separated in the second separatory funnel. Conversely, the upper phase was mixed with solvent B and separated using the first separatory funnel. This process of phospholipid isolation was repeated six times. The upper and lower phases obtained from the second separatory funnel were evaporated (50°C, 60 rpm). The upper phase of the second separatory funnel consists of the nonpolar extract, which contains a technical *n*-hexane solvent. The lower phase, on the other hand, contains CocoPLs. This study utilizes CocoPLs to make cocoliposomes that will encapsulate VEA.

2.3 Preparation of the VEA standard curve

A 200 ppm concentration stock solution of VEA was prepared by dissolving 10 mg of VEA p.a. in 50 mL of 0.1 M phosphate-buffered saline (PBS) solution at pH 7.4. The stock solution was diluted to concentrations of 0, 20, 40, 60, 80, 100, 120, 140, 160, 180, and 200 ppm. UV-Vis spectrophotometry was employed to determine the maximum wavelength of VEA. A series of diluted VEA solutions were used to generate the standard curve.

2.4 Encapsulation of vitamin E acetate within cocoliposomes (VEACL)

The term used to refer to the encapsulated VEA within cocoliposomes is VEACL. Table 1 presents five VEACL formulations consisting of CocoPLs, Chol p.a., and VEA p.a.

Table 1: Formulation of VEACL stock solution in 100 mL

VEACL formulation	Composition (w/w/w; mg)		
	CocoPLs	Chol p.a.	VEA p.a.
VEACL–0%Chol	125	0	2.5
VEACL–10%Chol	125	12.5	2.5
VEACL–20%Chol	125	25	2.5
VEACL–30%Chol	125	37.5	2.5
VEACL–40%Chol	125	50	2.5

For each formulation, the three compositions were dispersed in 100 mL of chloroform p.a.:methanol p.a. (in a ratio of 9:1, v/v). However, only 10 mL of the dispersion was used for the 1× encapsulation process. A volume of 10 mL of the dispersion was placed in a test tube to undergo the sequential steps of liposome preparation, which included thin film formation, hydration, freeze–thaw, and sonication. The tube was flowed with nitrogen gas, leaving only a thin layer at the bottom of the tube, and then 10 mL of PBS solution at pH 7.4 was added. Next, the freeze–thaw cycle was performed, which included heating the sample to 50°C, cooling it to 4°C, and vortexing it until the thin layer was dissolved. Subsequently, the dispersion was sonicated at 10% power for 3 min. These steps were replicated to generate liposomes without the addition of VEA, serving as a reference solution.

2.5 Functional group analysis

This study investigated the changes and interactions among CocoPLs, Chol p.a., and VEA p.a. that may occur during encapsulation using a Spectrum Two™ FTIR spectrophotometer (PerkinElmer®, MA, USA) in the spectral range of 5,500–435 cm^{-1} and a spectral resolution of 0.5 cm^{-1}. Tests were conducted on every component and mixture, precisely a mixture of CocoPLs, Chol p.a., and VEA p.a. The components were mixed in equal proportions, with a mass ratio of 1:1:1 (w/w/w).

2.6 Thermal analysis

Thermal analysis was performed using a differential scanning calorimeter (DSC; DSC-60 Plus Shimadzu®, Kyoto, Japan) in the temperature range of −20 to 200°C at a heating rate of 10°C/min and nitrogen gas airflow. This study investigated the phase changes resulting from the addition of substances into the system by observing the changes in physical and thermal properties. Tests were carried out on every component and mixture, precisely a mixture of CocoPLs with Chol p.a., CocoPLs with VEA p.a., and CocoPLs with Chol p.a. and VEA p.a. The components were mixed in equal proportions, with a mass ratio of 1:1:1 (w/w/w).

2.7 EE

The efficacy of the encapsulation process was assessed based on the extent to which liposomes successfully encapsulate the drug, as defined by the EE. The EE was determined using Ribeiro's method [23]. The dispersed liposome solution was centrifuged at 6,000 rpm for an hour. The supernatant was tested for the EE of VEA p.a. using a Shimadzu® UV-1280 multipurpose ultraviolet-visible (UV-Vis) spectrophotometer (Kyoto, Japan) at 288 nm. The EE value of VEA p.a. was determined by calculating the concentration of unencapsulated VEA p.a. (C_u) and comparing it with the initial concentration of VEA p.a. (C_0), as follows:

$$\text{EE\%} = \frac{C_0 - C_u}{C_0} \times 100\%, \tag{1}$$

where C_0 is the initial concentration of VEA p.a., and C_u is the concentration of unencapsulated VEA p.a.

2.8 Release rate (RR)

The RR was determined using the methodology described by Hudiyanti et al. [43]. The VEACL obtained from encapsulation was placed into a sealed vial and stored in the refrigerator. The concentration of VEACL released into the PBS solution was evaluated on 0, 1, 2, 3 to 8 days using a centrifugation process followed by supernatant testing using the above UV-Vis specifications at a wavelength of 288 nm. The RR was determined by dividing the C_u with the total release time (T_{tot}), which is 8 days, as follows:

$$\text{RR} = \frac{C_u}{T_{tot}} \times \frac{\text{ppm}}{\text{day}}. \tag{2}$$

2.9 Particle size and zeta potential analysis

The size and dispersity of the liposomes were evaluated using the particle size, while their surface charge was assessed using the zeta potential. The Horiba Scientific® nanoPartica SZ-100V2 Series nanoparticle analyzer (Kyoto, Japan) was used to assess the particle size and zeta potential of VEACL–0%Chol and VEACL–20%Chol.

3 Results and discussion

3.1 Functional group analysis with FTIR

FTIR-assisted functional group analysis is a chemical analysis method used to identify chemical compounds by analyzing the infrared spectrum they produce [44]. This method is precious for identifying the functional groups present in both organic and inorganic compounds [45]. Figure 1 displays the FTIR spectra for VEACL, VEA, Chol, and CocoPLs.

The spectra of CocoPLs exhibit distinct peaks at wavenumbers ($\tilde{\nu}$) = 2924.09 cm^{-1} (CH_2 asymmetric stretching), 2854.65 cm^{-1} (CH_2 symmetric stretching), 1743.5 cm^{-1} (C═O stretching), 1467.5 cm^{-1} (CH_2 scissoring), 1458.1 cm^{-1} (CH_3 asymmetric bending), 1373.32 cm^{-1} (CH_3 symmetric bending), 1234.44 cm^{-1} (PO_2^- asymmetric stretching), 1,165 cm^{-1} (CO–O–C asymmetric stretching), 1103.28 cm^{-1} (PO_2^- symmetric stretching), 1072.5 cm^{-1} (CO–O–C symmetric stretching), 972.12 cm^{-1} ($(CH_3)_3N^+$ symmetric stretching), 887.26 cm^{-1} (P–O asymmetric stretching), and 725.23 cm^{-1} (CH_2 wobble) [46].

The spectra of Chol exhibit distinct peaks at ($\tilde{\nu}$) = 3398.25 cm^{-1} (O–H stretching), 2935.5 cm^{-1} (CH_2 and CH_3 asymmetric stretching), 2,901 cm^{-1} (CH_2 symmetric stretching), 1667.75 cm^{-1} (C═C stretching), 1465.25 cm^{-1} (CH_2 and CH_3 symmetric stretching), 1377.5 cm^{-1} (CH_2 and CH_3 bending), 1054.5 cm^{-1} (ring deformation in C–H plane bending), 840.33 cm^{-1} (C–C–C stretching), and 700.67 cm^{-1} (═C–H) [43].

The spectra of VEA exhibit distinct peaks at ($\tilde{\nu}$) = 2866.8 cm^{-1} (C–H stretching), 1758.66 cm^{-1} (C═O stretching), 1460.27 cm^{-1} (CH_2 bending), and 1057.73 cm^{-1} (C═O stretching).

The spectra of VEACL exhibit distinct peaks at ($\tilde{\nu}$) = 2923.69 cm^{-1} (CH_2 asymmetric stretching), 2853.91 cm^{-1} (CH_2 symmetric stretching), 1741.04 cm^{-1} (C═O stretching), 1476.44 cm^{-1} (CH_2 scissoring), 1459.42 cm^{-1} (CH_3 asymmetric bending), 1374.56 cm^{-1} (CH_3 symmetric bending), 1204.03 cm^{-1} (PO_2^- asymmetric stretching), 1164.31 cm^{-1} (CO–O–C asymmetric stretching), 1100.85 cm^{-1} (PO_2^- symmetric stretching), 1072.57 cm^{-1} (CO–O–C symmetric stretching), 975.55 cm^{-1} ($(CH_3)_3N^+$ symmetric stretching), 801 cm^{-1} (P–O asymmetric stretching), and 723.04 cm^{-1} (CH_2 wobble) belong to CocoPLs, 3225.41 cm^{-1} (O–H stretching), 2923.69 cm^{-1} (CH_2 and CH_3 asymmetric stretching), 2853.91 cm^{-1} (CH_2 symmetric stretching), 1657.63 cm^{-1} (C═C stretching), 1463.85 cm^{-1} (CH_2 and CH_3 symmetric stretching), 1374.56 cm^{-1} (CH_2 and CH_3 bending), 1049.63 cm^{-1} (ring deformation in C–H plane bending), 923.46 cm^{-1} (C–C–C stretching), and 643.12 cm^{-1} (═C–H) belong to Chol, and 2868.94 cm^{-1} (C–H stretching), 1741.04 cm^{-1} (C═O stretching), 1452.86 cm^{-1} (CH_2 bending), and 1061.3 cm^{-1} (C═O stretching) belong to VEA.

Upon thorough analysis of all spectra, it was determined that the FTIR spectra of VEACL do not exhibit any new distinctive peaks that are not present in the individual spectra of CocoPLs, Chol, and VEA. This suggests that no chemical reactions occurred during the encapsulation of VEA in cocoliposomes. The absence of chemical processes is an important factor in the encapsulation process using liposomes because it will facilitate the easy release of drugs.

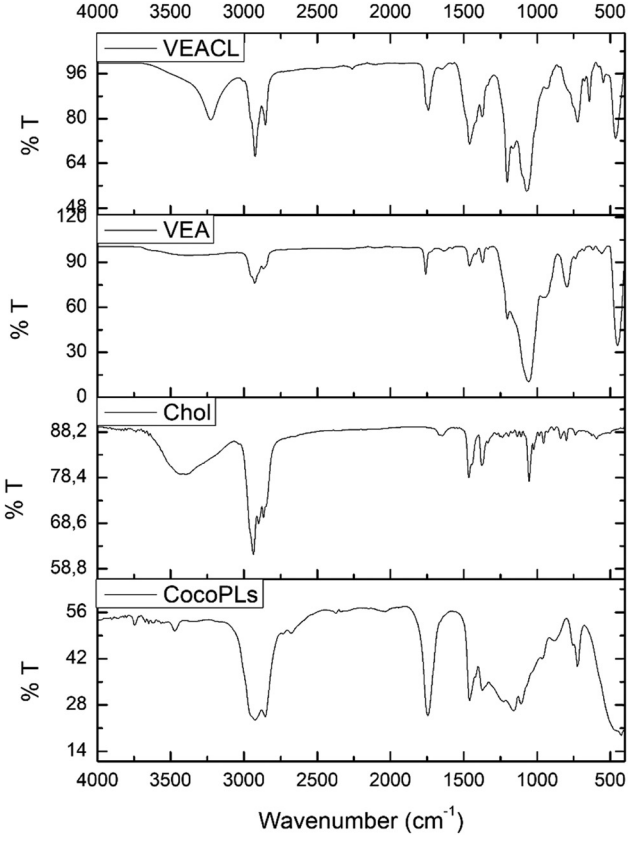

Figure 1: FTIR spectra for VEACL, VEA, Chol, and CocoPLs.

3.2 DSC thermal analysis

The data obtained from a DSC, commonly referred to as a DSC thermogram, are crucial for understanding the thermal properties of the material that is being investigated, including parameters such as the phase transition temperature (T_m), enthalpy, and thermal stability. The transition of most lipids from the gel phase (Lb') to the liquid crystal phase (La) is significant. The simultaneous melting of the hydrocarbon chains causes DSC peaks to have a high enthalpy, which signifies a rapid and reversible transition [47,48].

Figure 2 displays the DSC thermograms obtained by the measurements of temperature and the heat released

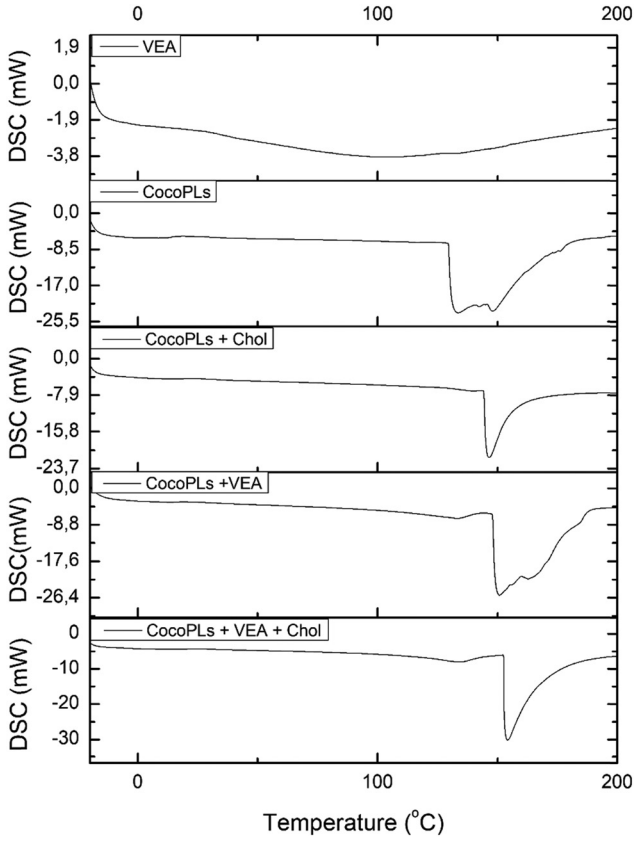

Figure 2: DSC thermograms for VEA, CocoPLs, CocoPLs + Chol, CocoPLs + VEA, and CocoPLs + VEA + Chol.

or absorbed by CocoPLs throughout the heating or cooling process. Three distinct peaks in the temperature range of 129.29–162.02°C suggest that the CocoPLs undergo a significant phase transition. All three peaks can be attributed to the existence of the CocoPLs as a mixture with a similar structure, resulting in phase transitions occurring at adjacent temperatures. The main phase transition occurs from the gel phase (Lb') to the liquid crystalline phase (La) at 133.64°C (T_m), which is considered to be the main T_m. The molecular structure and order of the CocoPLs undergo a transformation from a gel state to a liquid crystalline state during this transition.

The study conducted in 2009 by de Meyer and Smit [49] stated that the inclusion of Chol can increase the main T_m of phospholipids. Changes in the structure of these phospholipid membranes and how phospholipids and Chol interact could influence the rigidity and arrangement of molecules within the membrane. Chol, which improves the thermal stability of the phospholipids, affects the physical and thermal properties of the liposomes. As a result, the main T_m is elevated to a higher value. The occurrence will transpire upon the addition of Chol to the CocoPLs mixture. When CocoPLs and Chol are combined in equal proportions (1:1), as shown by the DSC thermogram in Figure 2, the gel phase (Lb) undergoes a transition to the liquid crystalline phase (La) at 144.04°C (T_m). These data demonstrate that including Chol in CocoPLs leads to an increase in the T_m [50].

Prior DSC thermograms of VEA exhibited three endothermic events that characterize the thermal behavior of this material. The first event is a stable state observed at temperatures up to 250°C, which suggests the occurrence of thermal decomposition in a single phase, subsequently leading to total decomposition. The other two events are identified at temperatures close to 300 and 400°C [51]. The events observed in the DSC thermogram generated by VEA in Figure 2 exhibit similarities to these events, and they remain stable even in the maximum temperature range. The next peak lies beyond the range of observation and hence cannot be observed.

Figure 2 shows the CocoPLs and VEA phase transitions determined using DSC thermal analysis. The pre-transition phase transformation from a gel phase with a planar structure to a rippling phase (Lb–Pb) occurs at 133.17°C (T_p). This phase transformation is followed by the main transition from a gel phase to a liquid crystalline phase (Lb–La) at 150.83°C (T_m). The inclusion of Chol has a direct effect on the elevation of T_m. When Chol is added, the planar-phase rippled gel (Lb'–Pb') pre-transition process occurs at 134.33°C (T_p), and the main transition from gel to liquid crystalline phase (Lb'–La') occurs at 154.19°C (T_m).

The thermogram data indicate that including Chol impacts the thermal properties and phase transitions in the CocoPLs and VEA mixture. These data indicate that the addition of Chol improves the mixture's thermal stability. This aligns with findings from other studies, indicating that liposomes constructed with phospholipids and cholesterol exhibit optimal longevity, with phase transition temperatures surpassing 37°C [36]. Furthermore, the absence of Chol does not significantly impact the first peak, indicating that the phase transition of CocoPLs and VEA at lower temperatures remains unaltered. Changes in the pre-transition and main transition temperatures signify alterations in the structure, whereas the inclusion of Chol is responsible for changes in the physical properties. This information is valuable for formulating CocoPLs, Chol, and VEA, especially in drug delivery or other applications requiring a better understanding of the thermal and phase properties of the system.

3.3 EE of VEACL

EE refers to the proportion of VEA successfully encapsulated within liposomes. The decreased ability of liposomes

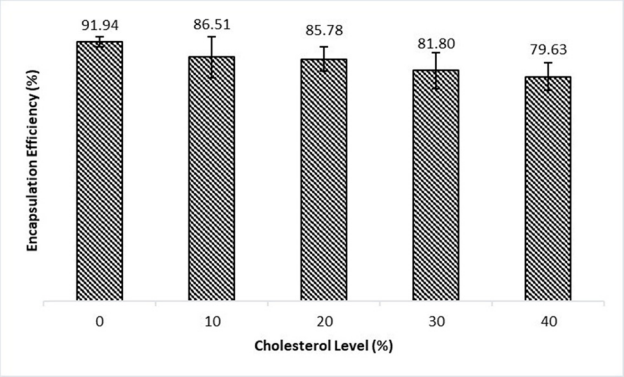

Figure 3: EE of VEACL.

to encapsulate VEA is evident from the decrease in the EE value. Figure 3 displays the results of the efficiency of the VEACL encapsulation process.

The efficacy of adding VEA into cocoliposomes depends on the Chol level, as indicated by the obtained data. Based on the findings shown in Figure 3, it can be observed that the EE of VEA decreased as the level of Chol increased. The efficiency of liposomes containing VEA was tested using different concentrations of Chol (0, 10, 20, 30, and 40%). The EE values obtained were 91.94 ± 1.66%, 86.51 ± 7.23%, 85.78 ± 4.35%, 81.80 ± 6.36%, and 79.63 ± 4.90%, respectively. The decrease in EE with increased Chol level is likely attributed to the competitive interaction between VEA and Chol for incorporation into the liposome membrane, as both molecules possess lipophilic properties.

The partition coefficient (log *P*), a measure of a compound's affinity for the lipophilic or hydrophilic phases, can be utilized to support these findings [52]. The position of each molecule in the liposomes can be calculated using the log *P* analysis. The lipophilic molecule will reside within the bilayer membrane (the nonpolar region of the liposome), while the hydrophilic molecule will be located within the aqueous compartment (the polar region of the liposome) [53]. The log *P* values determined using the Marvin Sketch calculation are presented in Table 2.

The locations of Chol and VEA on the membrane can be estimated, as depicted in Figure 4. Due to their lipophilic nature, VEA and Chol compete for the same area within the liposome bilayer membrane. Adding Chol can decrease the EE of VEA. The statement above concerning the location of both substances within liposomes is by their respective log *P* values. From a structural perspective, Chol is more manageable to occupy the liposome membrane than VEA. The O–H (hydroxyl group, polar) of Chol is usually located near the head group of phospholipids. In contrast, the nonpolar group of Chol is often situated near the tail group of phospholipids. Based on the comparison of log *P* values, where the log *P* value obtained from VEA is higher than the log *P* value obtained from Chol, it may be inferred that VEA is more likely to be among the phospholipid tail groups. Thus, the inclusion of Chol reduces the available area for VEA encapsulation, leading to a decrease in the EE value.

Increasing Chol levels in the liposomes reduces the EE of VEA, but the decrease is relatively small. Increasing the Chol level to 40% still provides a relatively high EE

Table 2: Partition coefficient (log *P*) values of Chol and VEA

Compound	Structure	log *P*	Nature
Chol	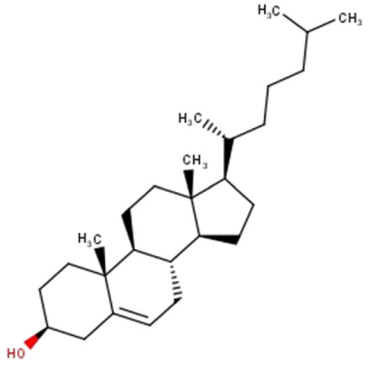	7.11	Lipophilic
VEA	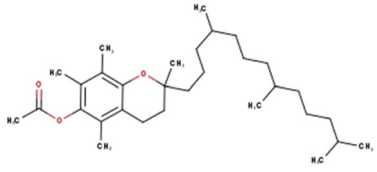	10.42	Lipophilic

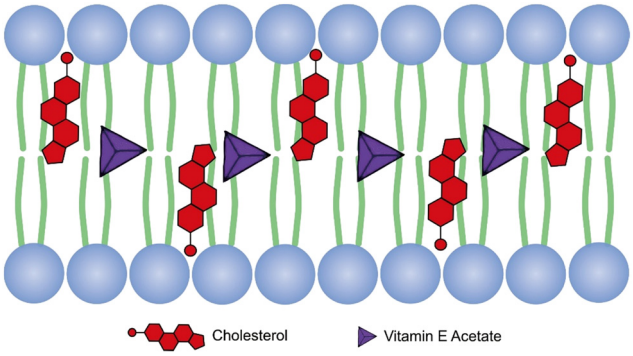

Figure 4: Approximate location of Chol and VEA in the liposomes.

percentage (above 80%). These data indicate that the addition of Chol does not have a significant effect on the EE of the VEACL system. Furthermore, these results are in line with the DSC results, where the presence of Chol can maintain the stability of the liposome structure. To understand the role and impact of Chol inclusion on cocoliposomes more completely, other analyses were carried out, such as RR, particle size, and zeta potential. Furthermore, studies concerning the stability and efficacy of VEA to assess its safety standards as a dietary supplement will be considered in future research.

3.4 RR of VEACL

This study aimed to assess the efficacy of liposomes maintaining the encapsulation of VEA by quantifying the amount of VEA released from liposomes over 8 days. In addition, the concentration of unencapsulated VEA was also analyzed to determine the degradation of VEA throughout the same period. The change in the concentration of unencapsulated VEA from day 1 to day 8 can be seen in Figure 5, with results showing a decrease of 25.75%. These data confirm that unencapsulated VEA degraded every day during the 8 days of observation. Therefore, VEA needs to be encapsulated to overcome this shortcoming.

The release profile serves as an assessment of the liposome's ability to be stored in VEA encapsulation. It is determined by the amount of VEA released into the external media surrounding the liposome over eight consecutive days. Figure 6 depicts the release profiles tested for VEACL–0%Chol and VEACL–20%Chol over 8 days. It can be seen that on day 8, the RR% for VEACL–0%Chol reached 72.53%, and VEACL–20% Chol reached 62.92%.

Liposomes containing Chol have a more uniform arrangement than liposomes without Chol. This occurrence could be attributed to the presence of Chol in liposomes, which effectively maintains the structural integrity of the liposomes and consequently reduces the leakage rate. Chol's location at the edge of the liposome membrane bilayer is believed to hinder the detachment of VEA from the membrane for a specific duration. The presence of Chol in liposomes induces stretching and regularity of fatty acid chains comprising phospholipids, causing the rigidification of the bilayer membrane. However,

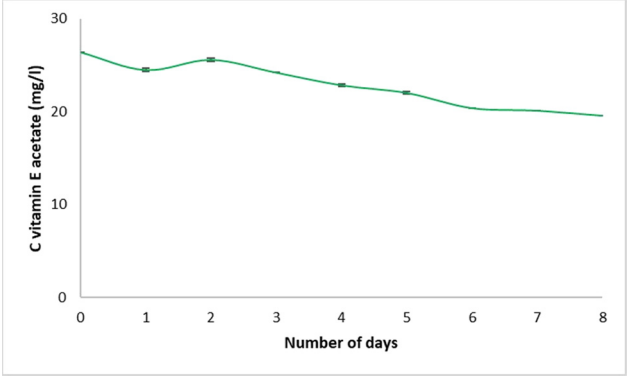

Figure 5: VEA degradation during 8 days of observation.

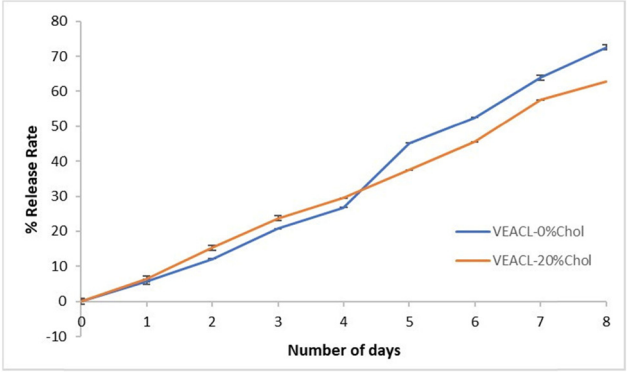

Figure 6: RR of VEACL during 8 days of observation.

Chol can sustain its fluidity to ensure stability [54], as confirmed by the release profile in Figure 6.

Figures 3 and 4 indicate that the cocoliposomes used in this study, together with the inclusion of Chol, succeed in encapsulating lipophilic drugs like VEA within their membrane bilayer with a relatively good percentage of EE. Figure 6 displays the influence of Chol on the inhibition of the RR of VEA encapsulated in cocoliposomes throughout an 8-day storage period. The findings depicted in Figure 3 demonstrate a negative correlation between the increase in the Chol level in cocoliposomes and the EE% of VEA. The cause of this occurrence is the competition between Chol and VEA when they are encapsulated in cocoliposomes (refer to Table 2 and Figure 4). Despite VEACL–20%Chol having a lower EE than VEACL–0%Chol, the addition of Chol is still advisable in the formulation since it will enhance liposome stability and reduce drug RR during storage (Figure 6). Therefore, it is crucial to consider the concentration of Chol incorporated while formulating liposomes, particularly for encapsulating lipophilic drugs, as it affects the EE and RR. Comparable outcomes were also reported by Adni and Ambi [55], where liposomes with a high cholesterol concentration (66.7%) yielded enhanced EE (83–85%), reduced liposome particle size (90−95 nm), and diminished RR over 24 h (50–52%), resulting in more controlled and prolonged drug delivery, and progressively negative zeta potential (−20 mV – (−22 mV)), indicating enhanced liposome stability. Furthermore, the study demonstrated that *in vivo*, liposomes with 66.67% cholesterol concentration exhibited the most significant tumor volume reduction in mouse models, achieving a reduction of 60–70% without inducing significant toxicity or adverse effects, as evidenced by histopathological analysis of major organs (liver, kidney, and spleen) [55].

3.5 Particle size and zeta potential analysis of VEACL

The stability of liposomes based on particle size, PI, and zeta potential was also studied. Stable liposomes can be seen from their small particle size, PI < 1.0, which reflects the homogeneity of the system, and a zeta potential that is more negative than ±30 mV. Therefore, the analysis of these three parameters was carried out in this study. The composition of the DDS, the interactions between those components, and the encapsulation method are all factors that influence the particle size [56]. Particle size analysis is one of the methods used to determine the average particle size and size distribution. Zeta potential is a parameter that quantifies the surface charge resulting from the ionization of chemical groups or the absorption of ions. The surface charge properties and composition of the dispersion have an impact on this parameter [57]. Table 3 shows the results of the analysis of the three parameters for the liposome system without Chol and with 20% Chol to determine the effect of Chol on liposome stability. Table 3 shows that VEACL–20%Chol exhibits smaller particle sizes compared to VEACL–0%Chol, where a smaller size of particles can be beneficial for enhancing absorption and effectiveness of drug delivery. VEACL–0%Chol exhibits an extensive particle size distribution or lacks concentration at a specific size, as indicated by the remarkably high PI value of 2.053 in the nanoparticle system. These data could be due to the liposomes undergoing aggregation due to the extended period between the creation of the samples and their testing. On the other hand, VEACL–20%Chol shows a PI value that is much lower than VEACL–0%Chol, namely 0.631. The PI value is a measure that quantifies the particle distribution inside a nanoparticle system [34]. PI in the range of 0.1–0.5 indicates a very concentrated or even distribution of particle sizes in the system, PI in the range of 0.5–0.7 indicates a rather even distribution of particle sizes in the system, and PI exceeding 0.7 indicates a very uneven particle size distribution in the system [35]. Therefore, obtaining a PI value <1 from VEACL–20%Chol indicates that the particle size distribution or homogeneity in the liposome system is quite good. The instability and agglomeration propensity of liposomes during storage is directly correlated with the size of PI. A very non-concentrated particle size distribution may indicate instability in the nanoparticle system [33]; therefore, it can be assumed that the liposome system with cholesterol has better stability and does not easily agglomerate during storage compared to the liposome system without cholesterol.

The zeta potential of liposomes can offer insights into the stability and behavior of the particles within the delivery system. Liposomes should possess a high zeta potential (exceeding +30 mV or falling below −30 mV). Under these circumstances, the liposomes will exhibit electrostatic stability due to their high surface charge, which hinders the aggregation of particles [58]. The zeta potential of VEACL–20%Chol was −34.7 mV, while VEACL–0%Chol was −12.3 mV. A higher or more negative zeta potential can enhance electrostatic stability and inhibit particle aggregation, increasing drug delivery efficacy [57]. Chol

Table 3: Particle size and zeta potential analysis in VEACL–0%Chol and VEACL–20%Chol

Variation	Particle size (nm)	PI	Zeta potential (mV)
VEACL–0%Chol	291.9	2.053	−12.3
VEACL–20%Chol	99.2	0.631	−34.7

can form negatively charged particles by creating a hydrogen bond between the hydroxyl group of the Chol head and the choline group or phosphate group of phosphatidylcholines. Due to this formation, the membrane attracts positively charged choline groups and negatively charged phosphatidyl groups. This action increases the negative charge and electrostatic repulsion of the particles [59]. The zeta potential data indicate that cholesterol in the liposome system is able to increase the stability of liposomes by increasing their surface charge, as indicated by the zeta potential value, which is below −30 mV.

3.6 Impact of cholesterol in encapsulated VEA

This study supports prior findings, showing that Chol influences the physicochemical properties of liposomes. Chol, with a planar and non-bulky molecular structure, which exhibits less steric hindrance within the liposome membrane, facilitates a condensing effect that promotes a tightly and orderly packed arrangement of phospholipids. A denser arrangement can yield a relatively smaller, more spherical, less permeable, and more rigid liposome membrane. This compact arrangement also contributes to improved stability and reduced leakage of the liposome during storage [60–63].

Furthermore, the binding calculation of a system comprising phospholipids, cholesterol, and VEA shows that Chol enhances interaction and stabilizes the bond, as seen by the reduced bond energy value for PC12…Chol…VEA interaction in Table 4.

These results align with *in vitro* analyses, which show that Chol's presence preserves liposome integrity by slowing down the leakage rate, consequently decelerating the RR (Figure 6). Further, it reduces liposome size due to enhanced interactions that shorten bond lengths (Table 3) and lower the PI value, as stronger interactions inhibit aggregation, resulting in a more stable distribution of particles within the liposome dispersion (Table 3).

Table 4: Binding energy among phospholipids (phosphatidylcholine (12:0); PC12), cholesterol, and VEA

Complex	Binding energy (kJ/mol)
PC12…PC12	−9.635
PC12…VEA	−12.012
PC12…Chol	−16.887
PC12…Chol…VEA	−19.916

4 Conclusions

This study successfully encapsulated VEA within cocoliposomes, referred to as VEACL, while studying the impact of adding Chol as a constituent component in the liposome system. The FTIR spectra of VEACL show no new distinct peaks that differ from the peaks of its constituent compositions. Therefore, it confirmed that no chemical reactions occurred during the synthesis of VEACL. Chol has several impacts on the VEACL system. It raises the transition temperature of phospholipids and enhances the stability of VEACL. Despite a 20% increase in cholesterol levels, the EE remains >80%. The RR of VEA from cocoliposomes was slower with VEACL–20%Chol compared to VEACL–0%Chol. Chol enhances the stability of VEACL due to its ability to decrease liposome size, improve the system's uniformity in particle size distribution, and provide an increasingly negative zeta potential value. The impacts of Chol on the VEACL system mentioned above highlight the need to carefully evaluate the Chol composition of liposome formulations used to encapsulate VEA.

Acknowledgments: DH, NN, AN, RIS, and IRA greatly acknowledged the support of the National Research and Innovation Agency (BRIN) and Educational Fund Management Institution (LPDP) through Innovation Research for Advanced Indonesia Research Scheme 2022.

Funding information: Financial support for this study was provided by the National Research and Innovation Agency (BRIN) and Educational Fund Management Institution (LPDP) through Innovation Research for Advanced Indonesia Research Scheme 2022 under Grant No. 947-05/UN7.D2/KS/XI/2022.

Author contributions: Conceptualization: DH; funding acquisition: DH, NN, AN, RIS, and IRA; methodology: DH and SNH; investigation: SNH, AN, RIS, IRA, ACP, and AEM; supervision: DH, PS, and NN; writing-original draft: DH and SNH; writing – review and editing: DH and SMC; resources: PS; project administration: SMC; formal analysis: SNH; validation: NN. All authors have read and agreed to the published version of this manuscript.

Conflict of interest: The authors declare no conflict of interest in the publication of this article.

Ethical approval: The conducted research is not related to either human or animal use.

Data availability statement: All data generated or analyzed during this study are included in this published article.

References

[1] Yang Y, McClements DJ. Vitamin E and vitamin E acetate solubilization in mixed micelles: Physicochemical basis of bioaccessibility. J Colloid Interface Sci. 2013;405:312–21.

[2] Keen MA, Hassan I. Vitamin E in dermatology. Indian Dermatol Online J. 2016;7(4):311–5.

[3] Cuerq C, Bordat C, Halimi C, Blond E, Nowicki M, Peretti N, et al. Comparison of α-tocopherol, α-tocopherol acetate, and α-tocopheryl polyethylene glycol succinate 1000 absorption by caco-2 TC7 intestinal cells. Nutrients. 2020;13(1):129.

[4] Concarr MJ, O'Rourke R, Murphy RA. The effect of copper source on the stability and activity of α-tocopherol acetate, butylated hydroxytoulene and phytase. SN Appl Sci. 2021;3(5):564.

[5] Zingg J-M. Vitamin E: A role in signal transduction. Annu Rev Nutr. 2015;35(1):135–73.

[6] Gianeti MD, Gaspar LR, Bueno de Camargo Júnior F, Berardo Gonçalves Maia Campos PM. Benefits of combinations of vitamin A, C and E derivatives in the stability of cosmetic formulations. Molecules. 2012;17(2):2219–30.

[7] Singh CD, Gohain AK, Bhuyan R, Dixit CP, Haloi S. Effect of supplementation of certain antioxidants (Vitamin E, vitamin C and selenium) on the growth performance of broiler chicken during heat stress. J Entomol Zool Stud. 2020;8(6):2066–71.

[8] Azad MAK, Kikusato M, Zulkifli I, Rahman MM, Ali MS, Hashem MA, et al. Comparative study of certain antioxidants-electrolyzed reduced water, tocotrienol and vitamin E in heat-induced oxidative damage and performance in broilers. Meat Res. 2021;1(1):1–5.

[9] Zhu C, Yang J, Nie X, Wu Q, Wang L, Jiang Z. Influences of dietary vitamin E, selenium-enriched yeast, and soy isoflavone supplementation on growth performance, antioxidant capacity, carcass traits, meat quality and gut microbiota in finishing pigs. Antioxidants. 2022;11(8):1510.

[10] Pereira R, Costa M, Velasco C, Cunha LM, Lima RC, Baião LF, et al. Comparative analysis between synthetic vitamin E and natural antioxidant sources from tomato, carrot and coriander in diets for market-sized Dicentrarchus labrax. Antioxidants. 2022;11(4):636.

[11] Zaaboul F, Liu Y. Vitamin E in foodstuff: Nutritional, analytical, and food technology aspects. Compr Rev Food Sci Food Saf. 2022;21(2):964–98.

[12] Raza R, Ahmad L, Saleemi MK, Arshad MI, Khatoon A, Soomro H, et al. Ameliorative effects of Vitamin E and Urtica dioica against thiamethoxam-induced teratogenicity in embryonated chicken eggs. Advancements Life Sci. 2023;10:577–84.

[13] Schmölz L, Birringer M, Lorkowski S, Wallert M. Complexity of vitamin E metabolism. World J Biol Chem. 2016;7(1):14–43.

[14] Flory S, Birringer M, Frank J. Bioavailability and metabolism of vitamin E. In: Weber P, Birringer M, Blumberg JB, Eggersdorfer M, Frank J, editors. Vitamin E in human health. Cham: Springer International Publishing; 2019. p. 31–41.

[15] Zareian S, Divsalar A, Irian S, Zarein F. Enrichment of food product with vitamin E using different encapsulation methods. Biomacromolecular J. 2020;6(1):9–16.

[16] Qureshi AA, Khan DA, Saleem S, Silswal N, Trias AM, Tan B, et al. Pharmacokinetics and bioavailability of annatto δ-tocotrienol in healthy fed subjects. J Clin Exp Cardiol. 2015;6:1–13.

[17] Smith DA, Beaumont K, Maurer TS, Di L. Volume of distribution in drug design. J Med Chem. 2015;58(15):5691–8.

[18] Toutain PL, Bousquet-Mélou A. Volumes of distribution. J Vet Pharmacol Ther. 2004;27(6):441–53.

[19] van Kempen TATG, Benítez Puñal S, Huijser J, De Smet S. Tocopherol more bioavailable than tocopheryl-acetate as a source of vitamin E for broilers. PLOS ONE. 2022;17(5):e0268894.

[20] Niki E, Abe K. Vitamin E: Structure, properties and functions. In: Niki E, editor. Vitamin E: Chemistry and nutritional benefits. London, UK: The Royal Society of Chemistry; 2019.

[21] Bodade RG, Bodade AG. Chapter 17 – Microencapsulation of bioactive compounds and enzymes for therapeutic applications. In: Pal K, Banerjee I, Sarkar P, Kim D, Deng W-P, Dubey NK, et al., editors. Biopolymer-based formulations. Amsterdam, Netherlands: Elsevier; 2020. p. 381–404.

[22] Chaves MA, Ferreira LS, Baldino L, Pinho SC, Reverchon E. Current applications of liposomes for the delivery of vitamins: a systematic review. Nanomaterials. 2023;13(9):1557.

[23] Ribeiro AM, Estevinho BN, Rocha F. The progress and application of vitamin E encapsulation – A review. Food Hydrocoll. 2021;121:106998.

[24] Aman Mohammadi M, Farshi P, Ahmadi P, Ahmadi A, Yousefi M, Ghorbani M, et al. Encapsulation of vitamins using nanoliposome: Recent advances and perspectives. Adv Pharm Bull. 2023;13(1):48–68.

[25] Gangurde AB, Ali MT, Pawar JN, Amin PD. Encapsulation of vitamin E acetate to convert oil to powder microcapsule using different starch derivatives. J Pharm Invest. 2017;47(6):559–74.

[26] Mujica-Álvarez J, Gil-Castell O, Barra PA, Ribes-Greus A, Bustos R, Faccini M, et al. Encapsulation of vitamins A and E as spray-dried additives for the feed industry. Molecules. 2020;25(6).

[27] Kiani A, Fathi M, Nasirpour A. Production of novel vitamin E loaded nanostructure lipid carriers and lipid nanocapsules for milk fortification. J Agric Sci Technol. 2021;23(3):545–58.

[28] Widayanti A, Elfiyani R, Lestari D. Effect of Lecithin's concentration of entrapment vitamin E acetate liposomes using thin layers hydration method. Adv Sci Lett. 2017;23(12):12510–3.

[29] Yang Y, McClements DJ. Encapsulation of vitamin E in edible emulsions fabricated using a natural surfactant. Food Hydrocoll. 2013;30(2):712–20.

[30] Han Y, Tai X, Liu H, Geng T, Yang X. Encapsulation of α-tocopherol acetate of emulsion gels by synergistic stabilization with polysaccharides and modified shea butter. New J Chem. 2023;47(37):17303–13.

[31] Phothong N, Aht-Ong D, Napathorn SC. Fabrication, characterization and release behavior of α-tocopherol acetate-loaded pH-responsive polyhydroxybutyrate/cellulose acetate phthalate microbeads. Int J Biol Macromol. 2024;260:129535.

[32] Liu P, Chen G, Zhang J. A review of liposomes as a drug delivery system: current status of approved products, regulatory environments, and future perspectives. Molecules. 2022;27(4):1372.

[33] Nsairat H, Khater D, Sayed U, Odeh F, Al Bawab A, Alshaer W. Liposomes: structure, composition, types, and clinical applications. Heliyon. 2022;8(5):e09394.

[34] Lee M-K. Liposomes for enhanced bioavailability of water-insoluble drugs: in vivo evidence and recent approaches. Pharmaceutics. 2020;12(3):264.

[35] Fan C, Feng T, Wang X, Xia S, John Swing C. Liposomes for encapsulation of liposoluble vitamins (A, D, E and K): Comparation of loading ability, storage stability and bilayer dynamics. Food Res Int. 2023;163:112264.

[36] Sambhakar S, Saharan R, Narwal S, Malik R, Gahlot V, Khalid A, et al. Exploring LIPIDs for their potential to improves bioavailability of lipophilic drugs candidates: A review. Saudi Pharm J. 2023;31(12):101870.

[37] Dymek M, Sikora E. Liposomes as biocompatible and smart delivery systems – the current state. Adv Colloid Interface Sci. 2022;309:102757.
[38] De Leo V, Milano F, Agostiano A, Catucci L. Recent advancements in polymer/liposome assembly for drug delivery: From surface modifications to hybrid vesicles. Polymers. 2021;13(7).
[39] Othman AK, El Kurdi R, Badran A, Mesmar J, Baydoun E, Patra D. Liposome-based nanocapsules for the controlled release of dietary curcumin: PDDA and silica nanoparticle-coated DMPC liposomes enhance the fluorescence efficiency and anticancer activity of curcumin. RSC Adv. 2022;12(18):11282–92.
[40] Abucayon EG, Sweeney S, Matyas GR. A reliable quantification of cholesterol and 25-hydroxycholesterol in liposomal adjuvant formulation by liquid chromatography high-resolution tandem mass spectrometry. ACS Omega. 2024;9(17):19637–44.
[41] Wu X, Dai X, Liao Y, Sheng M, Shi X. Investigation on drug entrapment location in liposomes and transfersomes based on molecular dynamics simulation. J Mol Modeling. 2021;27:111.
[42] Hudiyanti D, Kamila N, Wardani F, Anam K. Coconut phospholipid species: isolation, characterization and application as drug delivery system. London, UK: IntechOpen Limited; 2020.
[43] Hudiyanti D, Al Khafiz MF, Anam K, Siahaan P, Suyati L. Assessing encapsulation of curcumin in cocoliposome: In vitro study. Open Chem. 2021;19(1):358–66.
[44] Nandiyanto ABD, Oktiani R, Ragadhita R. How to read and interpret FTIR spectroscope of organic material. Indone J Sci Technol. 2024;4(1):97–118.
[45] Dutta A. Chapter 4 – fourier transform infrared spectroscopy. In: Thomas S, Thomas R, Zachariah AK, Mishra RK, editors. Spectroscopic methods for nanomaterials characterization. Amsterdam, Netherlands: Elsevier; 2017. p. 73–93.
[46] Hudiyanti D. Fosfolipida: Biosurfaktan. Yogyakarta, Indonesia: Deepublish; 2018.
[47] Lewis RN, McElhaney RN, Harper PE, Turner DC, Gruner SM. Studies of the thermotropic phase behavior of phosphatidylcholines containing 2-alkyl substituted fatty acyl chains: a new class of phosphatidylcholines forming inverted nonlamellar phases. Biophys J. 1994;66(4):1088–103.
[48] Garidel P, Johann C, Blume A. Non-ideal mixing and fluid–fluid immiscibility in phosphatidic acid–phosphatidylethanolamine mixed bilayers. Eur Biophys J. 2011;40(7):891–905.
[49] de Meyer F, Smit B. Effect of cholesterol on the structure of a phospholipid bilayer. Proc Natl Acad Sci. 2009;106(10):3654.
[50] Eric AS, Phoebe KD. Differential scanning calorimetry studies of phospholipid membranes: the interdigitated gel phase. In: Amal Ali E, editor. Applications of calorimetry in a wide context. Rijeka: IntechOpen; 2013. p. 18.
[51] Almeida MM, Lima CR, Quenca-Guillen JS, Moscardini Filho E, Mercuri LP, Santoro MI, et al. Stability evaluation of tocopheryl acetate and ascorbyl tetraisopalmitate in isolation and incorporated in cosmetic formulations using thermal analysis. Brazilian. J Pharm Sci. 2010;46:129–34.
[52] Silakari O, Singh P. ADMET tools: Prediction and assessment of chemical ADMET properties of NCEs. Concepts and experimental protocols of modelling and informatics in drug design; 2021. p. 299–320.
[53] Rothwell JA, Day AJ, Morgan MRA. Experimental determination of octanol−water partition coefficients of quercetin and related flavonoids. J Agric Food Chem. 2005;53(11):4355–60.
[54] Nogueira E, Gomes AC, Preto A, Cavaco-Paulo A. Design of liposomal formulations for cell targeting. Colloids Surf B: Biointerfaces. 2015;136:514–26.
[55] Adni M, Ambi N. Optimization of liposome formulations for enhanced bioavailability of hydrophobic drugs. J Adv Pharm Res Sci Sustainability (JAPRSS). 2024;1(1):46–57.
[56] Lengyel M, Kállai-Szabó N, Antal V, Laki AJ, Antal I. Microparticles, microspheres, and microcapsules for advanced drug delivery. Sci Pharm. 2019;87(3):20.
[57] Shah R, Eldridge D, Palombo E, Harding I. Optimisation and stability assessment of solid lipid nanoparticles using particle size and zeta potential. J Phys Sci. 2014;25(1):59–75.
[58] Duffy J, Larsson M, Hill A. Suspension stability; why particle size, zeta potential and rheology are important. Annu Trans Nordic Rheol Soc. 2012;20:209–14.
[59] Najaf Najafi M, Arianmehr A, Sani AM. Preparation of barije (ferula gummosa) essential oil–loaded liposomes and evaluation of physical and antibacterial effect on escherichia coli O157:H7. J Food Prot. 2020;83(3):511–7.
[60] Nasr G, Greige-Gerges H, Elaissari A, Khreich N. Liposome permeability to essential oil components: a focus on cholesterol content. J Membr Biol. 2021;254(4):381–95.
[61] Chen C, Tripp CP. A comparison of the behavior of cholesterol, 7-dehydrocholesterol and ergosterol in phospholipid membranes. Biochim Biophys Acta (BBA) – Biomembr. 2012;1818(7):1673–81.
[62] Song F, Chen J, Zheng A, Tian S. Effect of sterols on liposomes: Membrane characteristics and physicochemical changes during storage. LWT. 2022;164:113558.
[63] Ramli NA, Ali N, Hamzah SHS, Yatim NI. Physicochemical characteristics of liposome encapsulation of stingless bees' propolis. Heliyon. 2021;7:e06649.